

Microemulsion-based antifungal gel delivery to nail for the treatment of onychomycosis: formulation, optimization, and efficacy studies

Bhaves S. Barot · Punit B. Parejiya · Hetal K. Patel · Dharmik M. Mehta · Pragna K. Shelat

Published online: 20 October 2012
© Controlled Release Society 2012

Abstract Onychomycosis is the most common nail disease affecting nail plate and nail bed. Onychomycosis causes onycholysis which creates cavity between the nail plate and nail bed, where drug formulations could be applied, providing a direct contact of drug with the nail bed facilitating drug delivery on the infected area. The purpose of the present study was to design and evaluate the potential of microemulsion-based gel as colloidal carrier for itraconazole for delivery into onycholytic nails for effective treatment of onychomycosis. Itraconazole-loaded microemulsions were prepared and optimized using D-optimal design. The microemulsion containing 6.24 % oil, 36 % Smix, and 57.76 % water was selected as the optimized batch (MEI). The globule size and drug loading of the optimized batch were 48.2 nm and 12.13 mg/ml, respectively. Diffused reflectance FTIR studies were performed to study drug–excipient incompatibility. Ex vivo permeation studies were carried out using bovine hoof and human cadaver skin as models for nail plate and nail bed, respectively. Microemulsion-based itraconazole gel (MBGI) showed better penetration and retention in human skin as well as bovine hoof as compared to commercial preparation (market formulation, MFI). The cumulative amount of itraconazole permeated from the MBGI after 12 h was $73.39 \pm 3.55 \mu\text{gcm}^{-2}$ which was 1.8 times more than MF. MBGI showed significantly higher ex vivo antifungal activity ($P < 0.05$) against *Candida albicans* and *Trichophyton rubrum* when compared to MFI. Stability

studies showed that MBGI was stable at refrigeration and room temperature for 3 months. It was concluded that drug-loaded gel could be a promising formulation for effective treatment of onychomycosis.

Keywords Onychomycosis · Microemulsion · Itraconazole · Bovine hoof · D-optimal design

Introduction

Onychomycosis is a most common nail disease which affects the nail plate and nail bed. It affects 14 % of the total world population [1] with an incidence of 5 % in India [2]. Onychomycosis accounts for 50 % of the total nail diseases. It is more prevalent in elders and socio-economically backward people [3]. Onychomycosis is caused by infection of dermatophytes viz. *Trichophyton rubrum* or non-dermatophytes molds. Yeasts (*Candida albicans*, *Candida parapsilosis*) are also responsible in some cases. Onychomycosis causes discoloration, thickening, and hardening of the nail. Toe nails are frequently affected than finger nails, due to their slower growth and more susceptibility to infections [4, 5].

Drug delivery systems for fungal infections in nail area have been widely studied during the last few years. Conventional treatment of onychomycosis consists of (a) topical and/or systemic antifungal drug delivery and (b) surgical or chemical nail avulsion or (c) combination of these. Antifungal drugs like itraconazole, miconazole, and ketoconazole have been used orally but they are not widely accepted due to hepatic side effects, high relapse rate, and long duration of treatment. Further, the topical therapy of onychomycosis has limited success due to poor permeability of topically applied drugs through the nail plate [6]; while nail avulsion has been

B. S. Barot (✉) · P. B. Parejiya · H. K. Patel · D. M. Mehta · P. K. Shelat
Department of Pharmaceutics,
K. B. Institute of Pharmaceutical Education and Research,
Kadi Sarva Vishwavidyalaya,
GH-6 Road, Sector – 23,
Gandhinagar 382023, India
e-mail: bhavesbarot83@gmail.com

painful and traumatic for the patients [7]. Alternatively, topical therapy of the drug into nail by iontophoresis has also been researched, but it is quite expensive to be affordable for the patients with lower socio-economic class [8–10].

In onychomycosis, fungal infection spreads throughout the nail plate and nail bed and it causes detachment of the nail bed from the nail plate (onycholysis) within 4–5 weeks post-affliction [11]. Onycholysis imposes a resistance to drug permeation from formulation applied on ventral (upper) side of nail plate to nail bed. The nail fungal infection could be treated more easily, if a formulation is applied in onycholytic nail cavity, where it could reside for the sufficient period of time such that the drug penetrates into the nail bed and nail plate to kill the fungus [11, 12]. This objective could be attained if the drug is loaded into a colloidal carrier for application.

Microemulsion was chosen as a colloidal drug delivery carrier in the present investigation owing to its several advantages over other colloidal carriers in terms of ease of preparation, high solubilization capacity for hydrophilic and lipophilic drugs, long-term stability, and improved dermal drug delivery [13]. Microemulsions are transparent and thermodynamically stable as their droplet size range from 10 to 100 nm and they do not coalesce [14, 15]. Microemulsions are composed of oil, surfactant, co-surfactant, and water in specific proportions. The ingredients of microemulsion could facilitate the permeation rate of the drug by reducing the diffusion barrier of the stratum corneum [16–18]. However, due to low viscosity of the microemulsions, their minimal retention in the affected part imposes a resistance in its widespread use in pharmaceutical industry [19]. It is important to prevent the drug loss due to draining out from the onycholytic cavity or reaching the systemic circulation. In order to circumvent these problems, the colloidal drug delivery carrier should be loaded in a gel base. Zhu et al. showed that penciclovir-loaded microemulsion-based gel has excellent sustained release capability and enhanced skin permeation and retention due to viscosity imparted by Carbomer 940 [20].

In order to establish the specified objective of retention of drug into nail cavity, it is important to perform the ex vivo permeation studies simulating the in vivo condition. Till date, avulsed human cadaver nail plates and nail clippings from healthy volunteers have been used as a model for onychomycotic nail plates [7, 21]. But human nail plates require specially designed permeation cells for the study and the current methods of investigating nail permeation from human nail plates are time consuming and difficult to perform [22]. Recently, bovine hooves have been used as a model for the infected human nails due to their easy availability and larger dimensions. Bovine hooves can be trimmed to get a thickness equivalent to human nails so that it can easily fit into conventional diffusion cells [23, 24].

In the present investigation, itraconazole (IT), a triazole antifungal agent was selected for the study which is active against dermatophytes, fungi, molds, and yeasts and is used for both oral and topical treatment of mycoses [25–27]. The objective of the present study was to develop microemulsion-based gel of itraconazole for the effective treatment of onychomycosis. The developed formulation should retain in the upper layers of the nail bed and nail plate for effective action. The formulation was optimized using mixture experimental design and its efficacy was evaluated employing performance related tests such as ex vivo permeation study and ex vivo antifungal study. Permeation studies were carried using bovine hoof and human cadaver skin as models for onychomycotic nail plate and nail bed to simulate the onycholytic nail condition.

Materials and methods

Materials

Itraconazole was obtained as a gift sample from Cadila Healthcare Ltd. (Ahmedabad, India). Isopropyl myristate (IPM) was received as a gift sample from Bombay Tablets Pvt. Ltd. (Gandhinagar, India). Olive oil, oleic acid, and castor oil were purchased from National Chemicals (Vadodara, India). Tween 20, Tween 80, propylene glycol, and Cremophor EL were purchased from Sigma Aldrich (Mumbai, India). Methanol was purchased from Baroda Chemicals Ltd. (Vadodara, India). Capmul MCM was received as gift from Abitec Corporation (Ohio, USA). Labrasol, Labrafac, and Transcutol P were obtained as gift samples from Gattefosse (Lyon, France). Carbopol 934P was purchased from Corel Pharma (Ahmedabad, India). *T. rubrum* (MTCC no. 296) and *C. albicans* (MTCC no. 3018) were procured from Institute of Microbial Technology (Chandigarh, India). Double distilled water was used throughout the study. All other chemical reagents and solvents used were of analytical grade.

Screening of components for microemulsions

In order to find out the most suitable oil phase, surfactant and co-surfactant for microemulsion, solubility of IT was determined in oils such as oleic acid, IPM, olive oil, castor oil, oleic acid+IPM (1:1); in surfactants including Tween 20, Tween 80, Labrasol, Labrafac, and Cremophor EL; and in co-surfactants like Capmul MCM, Transcutol P, and propylene glycol. Excess amount of IT was added in 3 ml of oil/surfactant/co-surfactant in 5-ml-capacity stoppered vials separately and the resultant mixture was mixed initially by vortex mixer. The vials were then shaken on magnetic stirrer (Remi Instruments, Mumbai) for 72 h followed by centrifugation (Remi centrifuge, Mumbai) at 10,000 rpm for 15 min. The supernatant was filtered through a 0.45- μ m

filter membrane and the concentration of IT in filtrate was determined by HPLC after appropriate dilution with methanol. Appropriately diluted solutions of oil, surfactants and co-surfactants in methanol were taken as blank. The components that showed highest solubility of IT were used for further studies. Further, the components that showed highest solubility were assessed for compatibility. The mixtures of chosen oil and surfactant were prepared at 1:3, 1:2, 1:1, 2:1, and 3:1, respectively. The mixtures were mixed for 5 min using a vortex mixer and were evaluated for the physical appearance (clarity and absence of opacity). Similarly, compatibility study between the selected co-surfactant and the mixed system of oil and surfactant was tested by preparing mixtures of co-surfactant and mixed system of oil and surfactant at 1:3, 1:2, 1:1, 2:1, and 3:1, respectively. The blends were assessed for physical appearance [28].

Construction of pseudo-ternary phase diagrams

Pseudo-ternary phase diagrams were constructed by employing aqueous titration method in order to get concentration range of components of microemulsion. The ratio of surfactant to co-surfactant (S_{mix}) was altered at 3:1, 2:1, 1:1, and 1:2. For the construction of pseudo-ternary phase diagram at each S_{mix} ratio, the oily mixtures containing oil, surfactant, and co-surfactant were prepared with volume ratio of oil to S_{mix} at 1:9, 2:8, 3:7, 4:6, 5:5, 6:4, 7:3, 8:2, and 9:1, respectively. Double distilled water was added drop by drop to the oil and S_{mix} mixture under magnetic stirring at ambient temperature. Transparent and clear microemulsion was taken as the end point of aqueous titration method. The concentrations of components were then calculated in order to plot the pseudo-ternary phase diagram (Fig. 1).

Preparation of IT-loaded microemulsions

From the pseudo-ternary phase diagrams, S_{mix} ratio with maximum microemulsion region was selected. Different proportions of oil and S_{mix} were mixed depending upon the design points of the mixture experimental design (Table 1). Itraconazole was dissolved in the mixture of oil and S_{mix} under magnetic stirring at ambient temperature. Appropriate amount of double distilled water was added drop wise to the oily mixture until clear and transparent microemulsion was obtained. The mixture was allowed to stabilize and attain the equilibrium with gentle magnetic stirring for 15–20 min. All microemulsions containing IT were then stored at ambient temperature.

Optimization of microemulsion formulation

The levels of experimental design could not be chosen arbitrarily, where the composition is a factor of interest

because the sum of all the fractions of components equals to unity. Classical experimental designs do not consider specific experimental constraints, and thus they will not have the better prediction power [29, 30]. For instance, the possible experimental runs are displayed by an equilateral triangle in a three-component mixture design, where the real value of the responses could be then represented as distance orthogonal to factor space. Moreover, the range covering the components is limited in the design space, which could be represented by irregular polyhedron delimited by extreme vertices. In such cases, D-optimal design would be appropriate, as maximum prediction power could be obtained in selected set of experimental runs, minimizing the variance associated with the estimates of the coefficients in the model [31].

In the present study, the levels of the three independent variables; oil (X_1), S_{mix} (X_2), and water (X_3) were chosen on the basis of pseudo-ternary phase diagrams and preliminary experiments. As higher amount of oleic acid and IPM causes irritation of skin, their maximum level was restricted to 10 % [32]. Oleic acid and IPM have been used up to maximum 10 % earlier for topical formulations without causing skin irritation [33, 34]. Hydration effect of stratum corneum has significant effect on the penetration of the drug into skin. But, our objective was to retain the drug into bovine hoof and the skin, so the water content was restricted to 80 %. The range of the components for the design was selected as follows:

$$\begin{aligned} 5\% &\leq X_1 \leq 10\% \\ 10\% &\leq X_2 \leq 40\% \\ 50\% &\leq X_3 \leq 80\% \end{aligned}$$

The globule size (nanometer; Y_1) and drug loading in microemulsions (Y_2) were selected as the dependent variables (responses). The globule size (Y_1) was determined using photon correlation spectroscopy (Zetasizer 1000 HS, Malvern Instruments, UK) at 25 °C. The loading of IT in microemulsion (Y_2) was determined by extracting IT in methanol, which was analyzed by HPLC. The plain microemulsion without drug with the same composition was taken as blank and the drug loading capacity was determined.

The Minitab® software (Version 16.1.1; Minitab Inc., USA) was employed to treat the responses. The software selected a set of candidate points as a base design consisting of factorial points (high and low level from the constraints on each factor), centers of edges, constraint plane centroids, axial check point, and an overall center point. The base design consisted of total 16 runs. Suitable mathematical models of the mixture design such as linear, quadratic, and special cubic models were analyzed by the software. Significance of the model was determined by comparisons of statistical parameters like standard deviation (SD), R^2 , adjusted R^2 , predicted

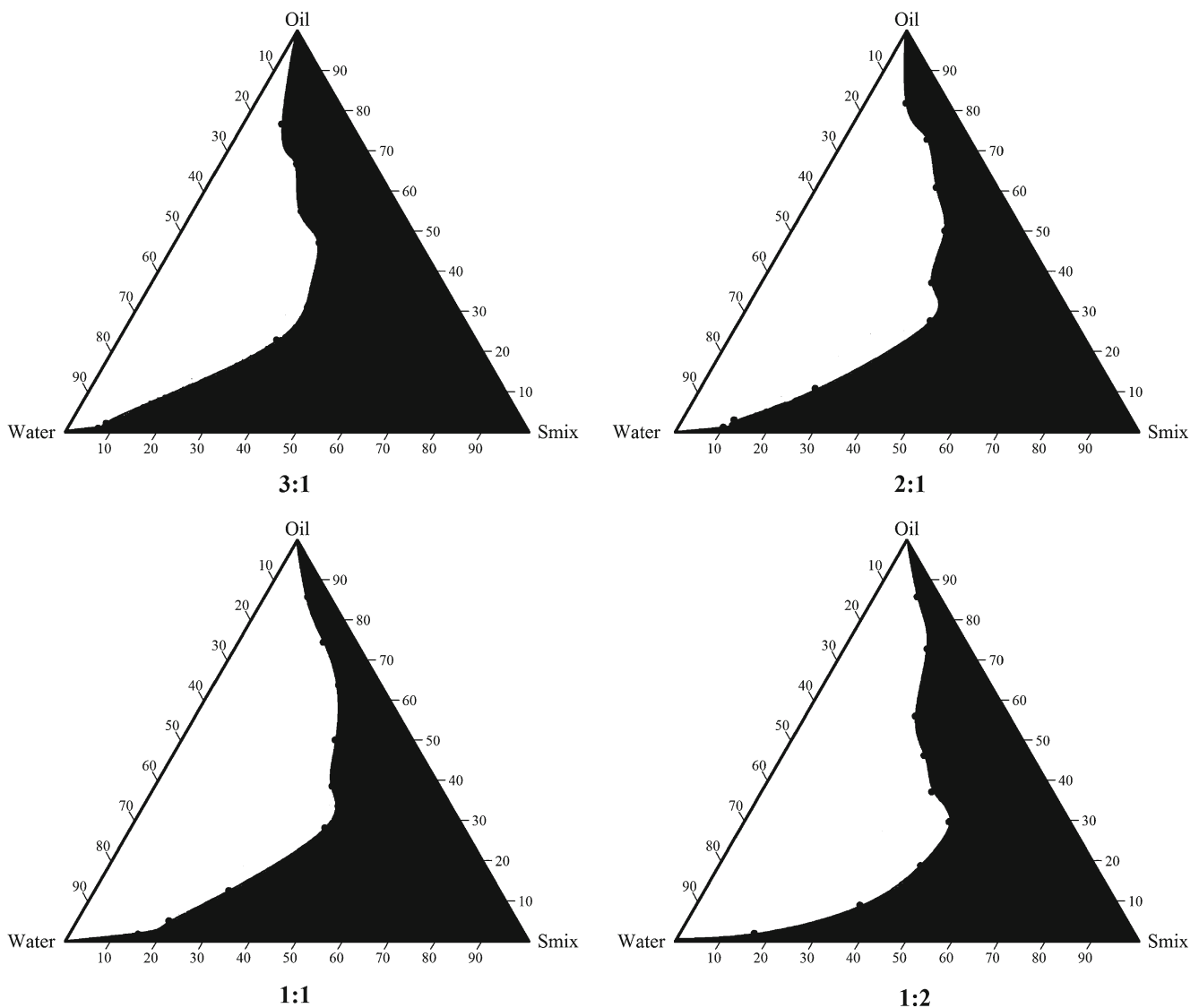


Fig. 1 Pseudo-ternary phase diagrams of MEs composed of oil (oleic acid+IPM (1:1)), Smix (surfactant: Labrasol, co-surfactant: Transcutol P), and water at various oil: Smix ratio (3:1, 2:1, 1:1, and 1:2)

R^2 , and predicted residual error sum of squares (PRESS). The best model was decided on the basis of higher values of adjusted R^2 and predicted R^2 . Moreover, the difference between adjusted R^2 and predicted R^2 should not be more than 0.2 in order to ensure the validity of the model. PRESS value should be small for the best model. PRESS demonstrates the excellence of model fitting. The optimum formulation was selected, which had the globule size (Y_1) less than 50 nm and drug loading (Y_2) between 12 and 16 mg/ml.

Formulation of microemulsion-based gel of IT

Microemulsions when applied in the cavity between the nail plate and nail bed, tends to drain out from the edges and hence the amount of drug reaching the target site would be quite less. Thus, the viscosity of microemulsions was required to be

increased with suitable gelling agent. Carbopol 934P was selected as a gelling agent due to its widespread use in pharmaceutical formulations and fast dispersion in water. Carbopol 934P was allowed to hydrate in sufficient quantity of water for 24 h at room temperature. Further, microemulsion with optimized components (MEI) was gradually added under magnetic stirring. The mixture was neutralized with triethanolamine until microemulsion-based gel (MBGI) with suitable consistency was formed. The final MBGI formulations contained 0.5 %, w/w IT.

Physicochemical characterization of microemulsions and its gel

The structure and morphology of MEI was studied using transmission electron microscopy (Tecnai 20, Philips,

Table 1 Runs of experimental design and their responses

Experimental runs	X_1	X_2	X_3	Y_1^a (nm)	Y_2^a (mg/ml)
1	1	0	0	89.34±1.53	15.59±1.51
2	0	1	0	33.67±1.53	11.41±1.03
3	0.4167	0.1667	0.4167	69±1.00	11.16±1.49
4	0.5	0	0.5	77.33±2.52	10.40±1.32
5	0.6667	0.1667	0.1667	75.67±1.53	14.02±0.29
6	0	1	0	33.33±1.53	11.32±1.10
7	0	0	1	59.67±1.15	7.28±1.05
8	0.5	0.5	0	72±2.00	12.45±1.34
9	0	0.5	0.5	75±1.00	11.38±1.10
10	0	0.5	0.5	72±1.00	12.17±1.65
11	0	0	1	62±1.00	7.52±0.74
12	0.1667	0.1667	0.6667	59.33±1.53	9.74±1.06
13	0.1667	0.6667	0.1667	45.67±1.53	12.49±1.00
14	0.5	0.5	0	67±1.00	13.31±1.28
15	0.4167	0.4167	0.1667	54±1.00	13.46±0.48
16	1	0	0	84.33±2.08	16.27±0.87

^aMean of 3±SD

Holland). One drop of appropriately diluted sample was directly deposited on holey film grid, was allowed to dry and examined under the microscope. The percentage transmittance of MEI was measured using UV spectrophotometer (UV 1800, Shimadzu Corp., Japan) at 650 nm. In order to ensure the encapsulation of IT in microemulsion, diffused reflectance infrared Fourier transform spectroscopy (DRIFTS) was carried out using Shimadzu Fourier transform infrared spectroscopy (FTIR; Shimadzu Inc., Japan). The samples were vacuum-dried before analysis. Itraconazole, MEI, and oil components were analyzed by potassium bromide disk method over scanning wavelength range of 4,000–400 cm^{-1} .

The refractive index of MEI was measured using Abbe refractometer (Bausch and Lomb, New York, USA) by placing one drop of MEI on the slide. Isotropic nature of microemulsions was verified by placing a drop of it on the glass slide with cover slip on it which was observed under cross polarized light using polarizing microscope (Carl Zeiss, Germany). Electrical conductivity of microemulsions was determined using a conductivity meter (CM-180 ELICO, India). The viscosities of MEI and MBGI were determined as such without dilution using Brookfield DV III Rheometer (Brookfield Engineering Labs, USA) with spindle LV III in 30 g samples using small sample holder. The pH of MEI was determined at 25 °C temperature using pH meter (Electroquip, Delhi). Stability studies of MEI and MBGI were performed as per International Conference on Harmonisation (ICH) guidelines at four different storage conditions (i.e., refrigeration, 25±2 °C/60±5 % RH, 30±2 °C/65±5 % RH, and 40 ±2 °C/67±5 % RH). The MEI samples were assessed

for globule size and polydispersity index (PDI) and MBGI samples were assessed for appearance after withdrawing them at predetermined time intervals of 3 and 6 months [35].

Ex vivo permeation studies

In onychomycotic nails, infection resides in both nail plate and nail bed. When onycholysis occurs during onychomycosis, a cavity is formed between the nail plate and nail bed where the gel could be applied. The applied gel would be in direct contact with both nail plate and nail bed. To simulate this condition, ex vivo permeation studies were carried out using human cadaver skin as a model for nail bed and bovine hooves as a model for onychomycotic human nail plate. The nail bed is a skin consisting of non-cornified soft tissue which is structurally similar to the skin of the foot region [36]. Bovine hooves are considered equivalent to infected human nails in predicting the in vivo efficacy of the drug products in nail diseases [37]. The experiments were performed after getting approval from Institutional Animal Ethics Committee of K. B. Institute of Pharmaceutical Education and Research (KBIPER), Gandhinagar, India (protocol no. KBIPER/2011/289). Full thickness dermatomed human cadaver skin from the foot region of Asian subjects was received from N.H.L. Municipal Medical College (Ahmedabad, India). The skin was stored in 10 % glycerin solution at temperature of –20 °C till the experiments were started. The skin was inspected for any holes or irregularities. Bovine hooves were obtained from freshly slaughtered cattle from Rancharda slaughter house (Ahmedabad, India). The hooves were made free

of attached cartilaginous and connective tissue and were soaked in 10 % formalin solution till they were cut into slices. Bovine hooves were sliced with a cryotome to 0.7–0.9-mm-thick membranes. The human cadaver skin and bovine hoof membranes were hydrated in acetate buffer for 1 h at room temperature before the permeation study.

A Franz diffusion cell with an effective diffusion area of 7.1 cm² was used for the experiment. The skin and bovine hoof membrane were cut in into 3.3×3.3-cm² area for the permeation study. The drug-loaded gel was placed between the bovine hoof membrane and the human cadaver skin. Further, the bovine hoof membrane and the skin were placed between the donor and receptor compartment of Franz diffusion cell such that bovine hoof membrane faces the donor chamber while the human cadaver skin faces the receiver chamber.

MEI (12.3 %, w/w IT), MBGI (0.15 %, w/w IT), and market formulation (MFI; 1 %, w/w IT) were taken equivalent to 20 mg IT and were placed between bovine hoof membrane and skin and the release profiles were taken. The receptor chamber was filled with 25 ml of physiological saline solution (pH5.5 acetate buffer/methanol (9:1)). The receptor medium was maintained at 37 ±1 °C and was magnetically stirred at 50 rpm. Samples were withdrawn at predetermined time intervals, filtered through a 0.45-μm pore size cellulose membrane filter and were analyzed by HPLC. Fresh buffer solution was immediately replaced into the receptor chamber after each sampling. Cumulative amount of drug in receptor chamber for the three formulations (MEI, MBGI, and MFI) was plotted as a function of time (*t*, h). The cumulative amount of IT permeated through the skin was determined as per the following equation:

$$Q_n = \frac{C_n \times V_0 + \sum_{i=1}^{n-1} C_i \times V_i}{S} \quad (1)$$

Where, C_n is the drug concentration of receptor medium after each sampling time, C_i is the drug concentration for *i*th sample, V_0 and V_i are the volumes of the receiver solution and sample, respectively, and S is the effective diffusion area [17].

Ex vivo antifungal study

The cylinder plate method was selected for the antifungal study. MFI and MBGI were evaluated for their antifungal activity using two fungal strains, *T. rubrum* (MTCC no. 296) and *C. albicans* (MTCC no. 3018). *T. rubrum* was cultivated on Sabouraud dextrose media (Himedia, India) at 25 °C for 7 days, while *C. albicans* was also cultivated on Sabouraud dextrose media at

30 °C for 2 days. The spores were harvested with spatula, and were suspended in 20 ml media and finally filtered through sterile gauze. Ten milliliters of the inoculated media was added to solidified agar media in the petri dish. Three wells in the petridish were bored and filled with 0.1 g each of MBGI and MFI; and control (distilled water). Two petridishes were used for two different strains. Petridish with *T. rubrum* was incubated at 25 °C for 7 days, while petridish containing *C. albicans* was incubated at 30 °C for 2 days. Zone of inhibition diameter (millimeter) was then recorded and compared. The experiments were performed in aseptic area.

HPLC analysis of IT

Itraconazole was analyzed by reverse phase HPLC (Supelco column 516, C18, 5 μm, 250×4.6 mm). The HPLC system (SCL-10 AVP, Shimadzu, Japan) consists a binary pump (LC-10 ATVP Shimadzu, Japan), and a UV detector (SPD-10 AVP, Shimadzu, Japan). The mobile phase was methanol/water (75:25 v/v) with a flow rate of 1.0 ml/min. The detection wavelength was set at 262 nm and the retention time was 3.5 min. The assay was linear in the concentration range of 10–50 μg/ml with a lowest detection limit of 0.05 μg/ml. The percentage recoveries ranged from 98.0 to 101.0 %. There was no interference in any of the formulation components. Aliquots of 10 μl were injected into the HPLC system via auto-injector. The samples were filtered through a 0.45-μm pore size membrane filter before injection [38].

Statistical analysis

Data were represented as mean±SD ($n=3$). Data were analyzed statistically by Student's *t* test at 5 % significance level using GraphPad Prism 5 program (GraphPad Inc., USA)

Results and discussion

Screening of components for microemulsion

The solubility of IT in various oils, surfactant, and co-surfactants was estimated for screening the components for microemulsions containing IT. Solubility of IT was highest in oleic acid+IPM (1:1; 140.01±4.22 mg/ml) among the four oils, followed by IPM alone (90.84±3.30 mg/ml) and oleic acid alone (63.14±2.94 mg/ml); while in olive oil, IT has the lowest solubility (17.95±0.98 mg/ml). Oleic acid+IPM (1:1) was selected for further study owing to its solubility profile. Moreover, oleic acid as well as IPM has the

potential to enhance the dermal permeation, as it renders increase in fluidity of the lipid portion of stratum corneum [39–41].

The solubility of IT was higher in Tween 80 (9.99 ± 1.17 mg/ml) and Labrasol (7.84 ± 0.37 mg/ml) among surfactants. However, results of compatibility studies showed that Tween 80 was not compatible with the selected oil phase in all proportions while Labrasol showed miscibility in all proportions with the oil phase. Hence, Labrasol was selected as a surfactant. It has been reported that surfactants could cause skin irritation, when applied topically. Hence, it is vital to use the surfactant as minimum as possible. Toxicity levels are relatively low for non-ionic surfactants like Labrasol [42]. Transcutol P demonstrated higher solubility of IT (30.5 ± 1.89 mg/ml) among the tested co-surfactants; hence it was selected for further study. The blends of mixed system of selected oil phase (oleic acid+IPM) and surfactant (Labrasol) with co-surfactant (Transcutol P) showed miscibility and transparency in all proportions. Globule separation and/or precipitate formation was not noticed during the experiments.

Construction of pseudo-ternary phase diagrams

In order to obtain the appropriate components and their concentration ranges for microemulsions, the pseudo-ternary phase diagrams were constructed for different Smix ratio, 3:1, 2:1, 1:1, and 1:2. The ratio which provided stable and clear solutions was selected. With the help of phase diagram, relationship between the phase behavior of its mixture and components could be explained. From the four phase diagrams (Fig. 1), the largest microemulsion region was observed in Smix 3:1. The microemulsion region showed the expansion as the proportion of Labrasol was increased, while in the phase diagrams with Smix ratio of 2:1, 1:1, and 1:2, the microemulsion region shows contraction. For the formation of microemulsions, the combination of surfactants with short- to medium-chain length alcohol (Transcutol P) is required for lowering the interfacial tension. The presence of short-chain alcohols helps in decreasing the bending stress of interface by making interfacial film sufficiently flexible to form different curvatures which are necessary for microemulsion formation over wide range of composition. However, increase in short-chain alcohol concentration causes decrease in microemulsion region (Smix ratio 2:1, 1:1, and 1:2) due to presence of low concentration of Labrasol, which inhibits micelle formation and subsequently results in decrease in drug solubilization capacity of microemulsions. Microemulsion formed with Smix ratio of 1:1 and 1:2 were highly unstable and showed phase separation within 12–14 h (data not shown). Thus, Smix ratio of 3:1 was selected for further optimization study [14, 42].

Optimization of microemulsion formulation

Table 1 shows the composition of 16 experimental runs. The responses (Y_1 : Globule size (nanometer) and Y_2 : drug

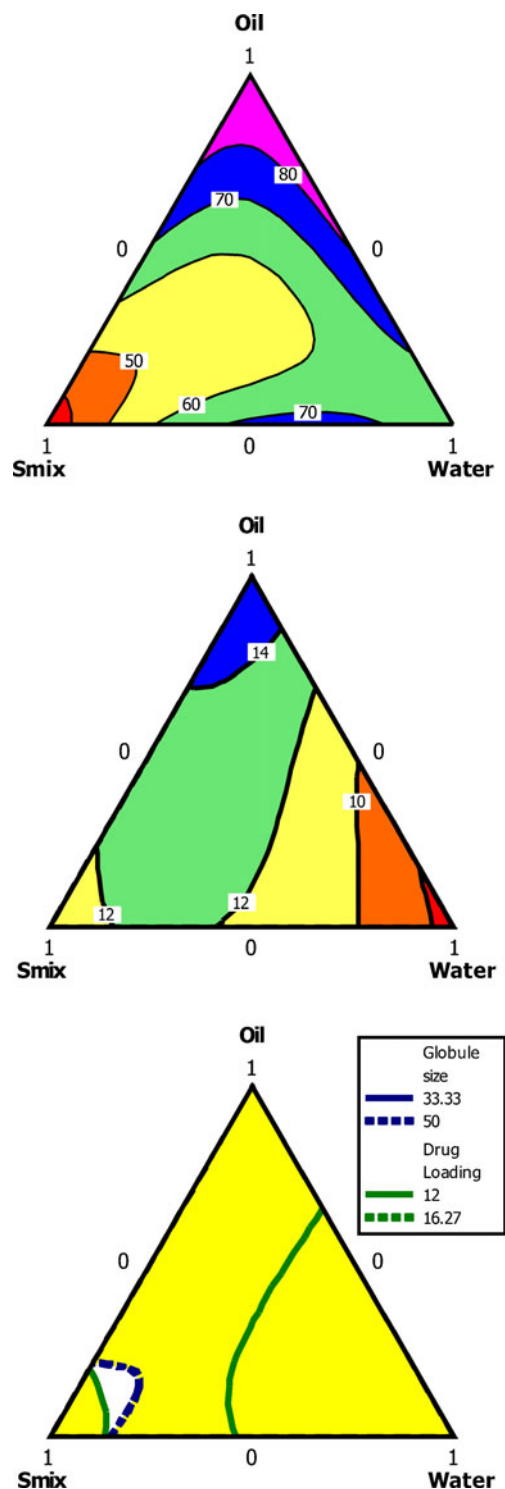


Fig. 2 Contour plots: **a** the effect of variables on globule size (Y_1), **b** effect of variables on drug loading (Y_2) **c** Overlay plot for the effect of variables on globule size (Y_1) and drug loading (Y_2)

Table 2 Model summary statistics of the measured responses

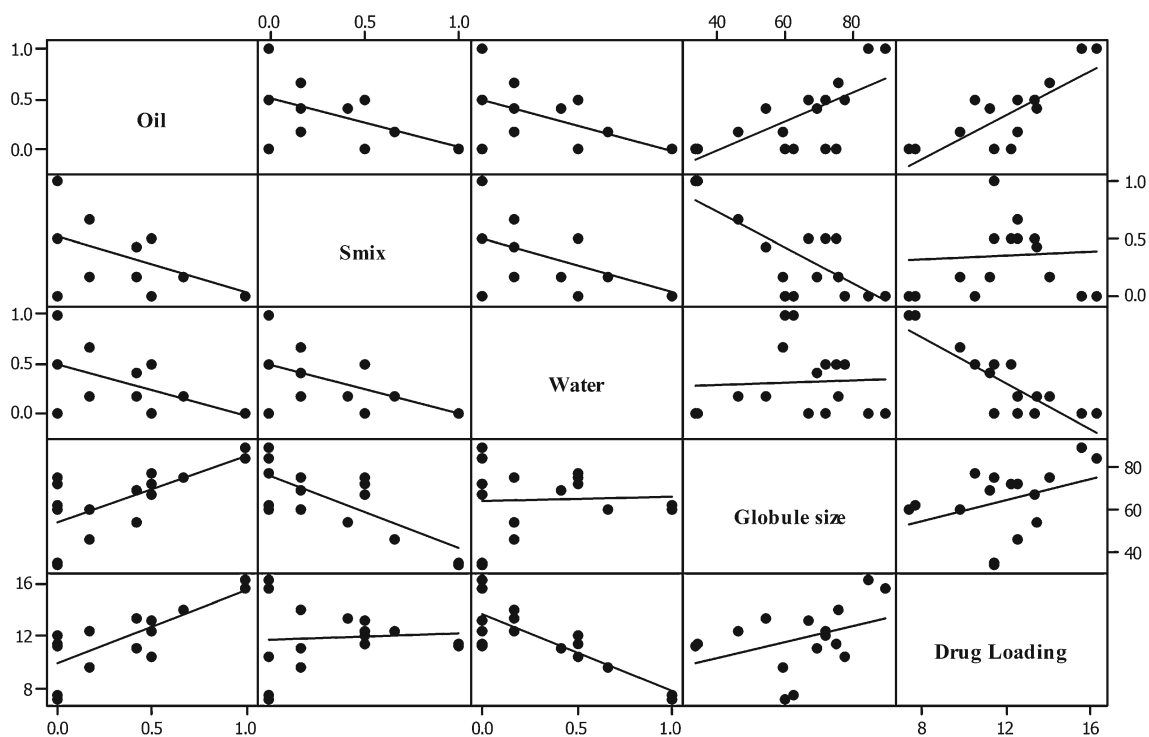
Response	Model	SD ^a	R ²	Adjusted R ²	Predicted R ²	PRESS
Y ₁	Linear	9.82	0.6861	0.6378	0.5553	1775
	Quadratic	7.78	0.8484	0.7726	0.6301	1476.64
	Special cubic	4.16	0.9609	0.9348	0.7889	842.44
	Cubic	3.51	0.9785	0.9538	0.701	1193.43
Y ₂	Linear	1.03	0.8492	0.826	0.7829	19.79
	Quadratic	0.49	0.9731	0.9597	0.9379	5.66
	Special cubic	0.47	0.9783	0.9638	0.9155	7.7
	Cubic	0.44	0.9854	0.9687	0.862	12.58

loading (milligram per milliliter)) were determined after 1 h of the microemulsion formation, in order to stabilize them. As shown in the table, lowest globule size (Y_1 , 33.33 nm) was obtained with run 2 (0, 1, 0; X_1 , 5 %; X_2 , 40 %; X_3 , 50 %), where proportion of oil was lowest while that of Smix was highest. It implies that as the proportion of oil decreases, the globules tend to constrict and get stabilized with maximum amount of Smix. The highest globule size was 89.33 nm. The wide range of globule size in the design space implies the effect of selected independent variables on the globule size. On the contrary, drug loading (Y_2) was highest when proportion of oil was at high level (run 16 (1, 0, 0); X_1 , 10 %; X_2 , 10 %; X_3 , 50 %). This is due to the increased amount of solvent necessary to solubilize the IT in the system. Graphical presentation of the data is easy to interpret and hence Fig. 2a, b was drawn to display the results.

The relationship between responses (dependent variables) and factors (independent variables) was established using quadratic equation through statistical analysis of the software, for determining the composition, which yields microemulsion formulation with ideal attributes. The equation that fitted to the data is as follows:

$$Y = \beta_1 X_1 + \beta_2 X_2 + \beta_3 X_3 + \beta_4 X_1 X_2 + \beta_5 X_1 X_3 + \beta_6 X_2 X_3 + \beta_7 X_1 X_2 X_3 \quad (2)$$

Where, β_1 to β_7 are the coefficients computed from the observed experimental values of Y . Coefficients with one factor represents the effect of that particular factor while the coefficients with more than one factor represents the interaction between those factors. Positive sign in front of the terms indicates synergistic effects while the negative sign indicates antagonistic effect of the factors. Model equations

**Fig. 3** Scatter plot matrix graph of experimental design formulations along with their responses (globule size and drug loading)

were calculated using the coded levels. Model equations were calculated, after converting the actual constraints into the coded levels ($0 \leq X_1, X_2, X_3 \leq 1$). The conversion was done to overcome the complexity of the non-simplex models, where one of the components (X_1) relatively varied less than the other two components (X_2 and X_3).

Table 2 represents the model summary statistics of the responses. For response Y_1 , special cubic model showed a superior fit while for response Y_2 , quadratic model showed superior fit. The fitted models of the responses showed higher values of adjusted R^2 and predicted R^2 and smaller values of PRESS than other models. Analysis of variance was carried out with the software to generate the polynomial equation of the responses. A factor is considered to influence the response, if the effects significantly deviate from zero and the p value is less than 0.05. For response Y_1 , factor X_1X_3 was not significant, while for response Y_2 , the factor X_1X_2 was not significant, as their p values were greater than 0.05. Equations 3 and 4 represent the refined regression equation of the responses which could be used to calculate the predicted values for other formulations in the design space.

$$Y_1 = 87.67X_1 + 32.71X_2 + 60.35X_3 + 34.87X_1X_2 + 102.34X_2X_3 - 631.48X_1X_2X_3 \quad (3)$$

$$Y_2 = 15.99X_1 + 11.36X_2 + 7.29X_3 - 4.25X_1X_3 + 10.11X_2X_3 \quad (4)$$

The globule size of microemulsion should be as small as possible to penetrate into the deeper layers of nail plate and nail bed. The contour plot of globule size (Y_1 ; Fig. 2a) proved that oil proportion needs to be lesser in amount to have the minimum globule size of microemulsion. The contour plot of drug loading (Fig. 2b) and Eq. 4 show that Smix has a very significant effect on the drug loading. It has been reported that retention of drug in the bovine hoof and skin depends on the distribution of drug between the vehicle of microemulsion and layers of keratin in bovine hoof and stratum corneum of skin [11, 43]. Thus, the composition of microemulsion showing highest drug loading would probably result into reduced partitioning into the skin layers and nail, and majority of the drug would be retained in the vehicle after application of the formulation. The scatter plot matrix graph of experimental design formulations and the two responses is shown in Fig. 3, which shows that oil and Smix are negatively correlated due to restrictive effect on each other for

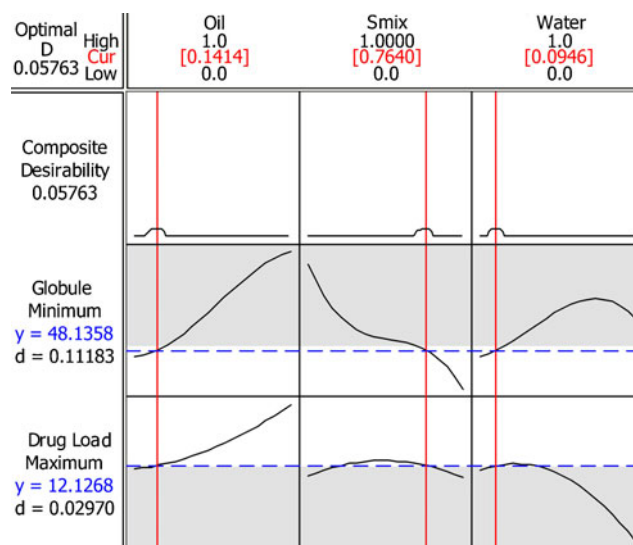


Fig. 4 Prediction profile optimizer plot

microemulsion formation. Further, the responses Y_1 and Y_2 shows moderately positive correlation which demonstrates that the formulation with one good or optimal response is likely to have other response close to ideal attributes.

The composition of microemulsion, providing the globule size (Y_1) less than 50 nm and the drug loading in microemulsion system (Y_2) between 12 and 16 mg/ml was considered as ideal. Figure 2c is the overlaid contour plot which shows the optimized region (white color) wherein all the batches inside that region will form the microemulsion with ideal attributes. The composition of the formulation with ideal attributes was selected through the prediction profile optimizer plot (Fig. 4) generated through the software. The factors X_1 , X_2 , and X_3 at 0.414, 0.7640, and 0.0946 levels, respectively, provided the optimum response of 48.13 nm and Y_2 : 12.12 mg/ml. The actual levels of X_1 , X_2 , and X_3 corresponding to optimized coded levels are 6.24 %

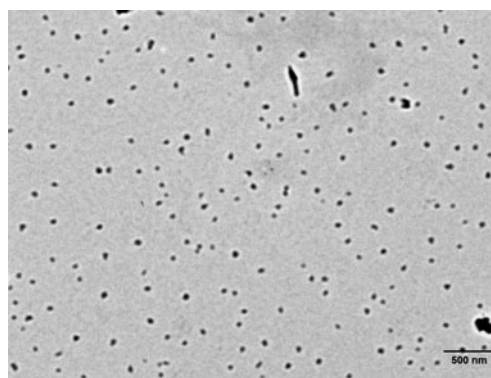
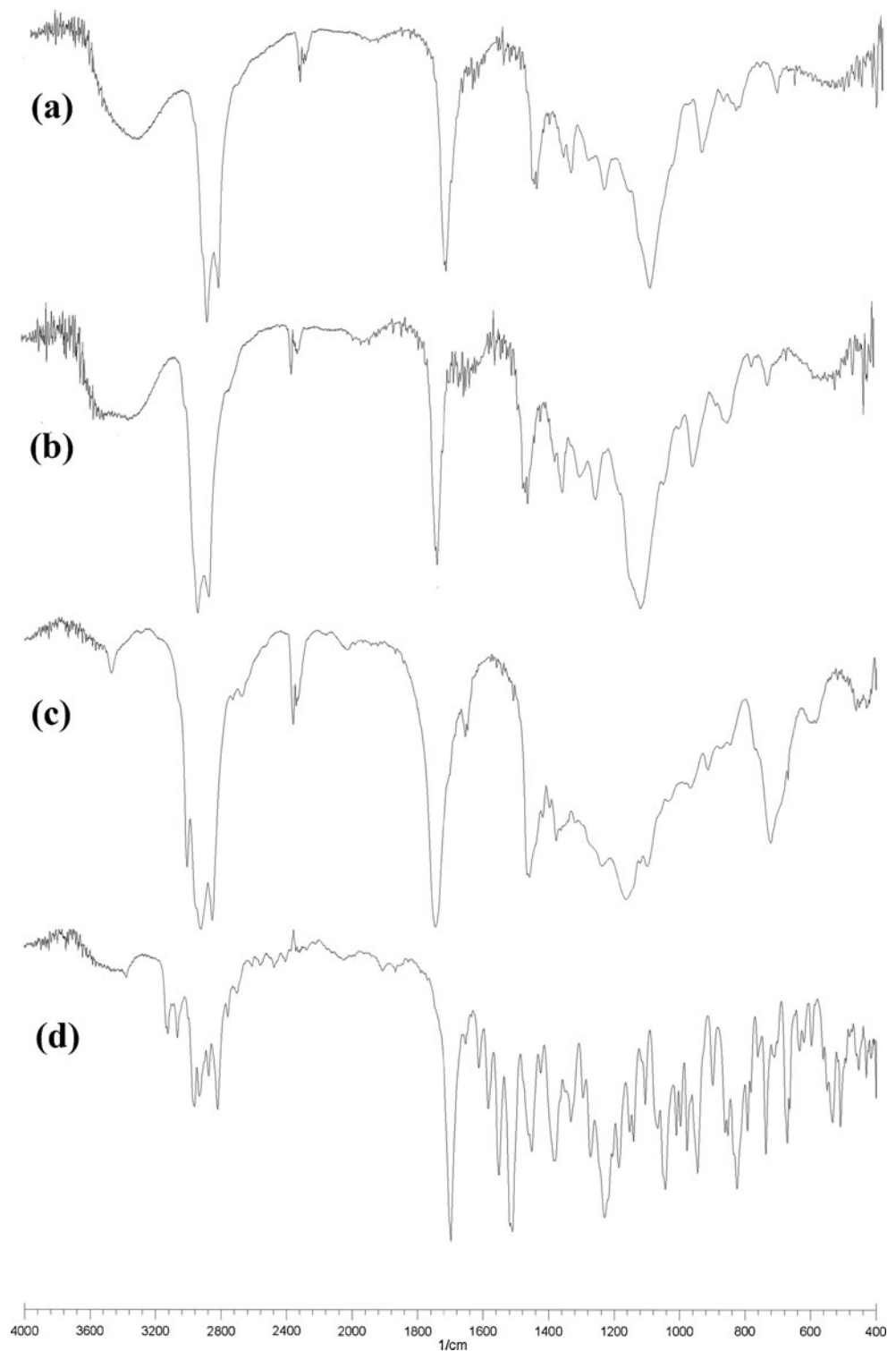


Fig. 5 TEM image of MEI

(oil), 36 % (Smix) and 57.76 % (water), respectively. In order to assess the reliability of the developed mathematical model, optimized microemulsion formulation (MEI) was formed corresponding to above mentioned factor levels. Experimental values of Y_1 and Y_2 for the optimized batch were 48.2 ± 2.62 and 12.3 ± 1.05 ,

respectively, while predicted values (calculated by equation) were 48.13 and 12.12, respectively. Percentage prediction error (PPE) was determined as 100th times the ratio of difference between the experimental value and predicted value to the experimental value. The magnitudes of PPE for Y_1 and Y_2 were 0.15 and 1.46,

Fig. 6 FTIR spectra of **a** itraconazole MEI, **b** IPM, **c** oleic acid, and **d** itraconazole

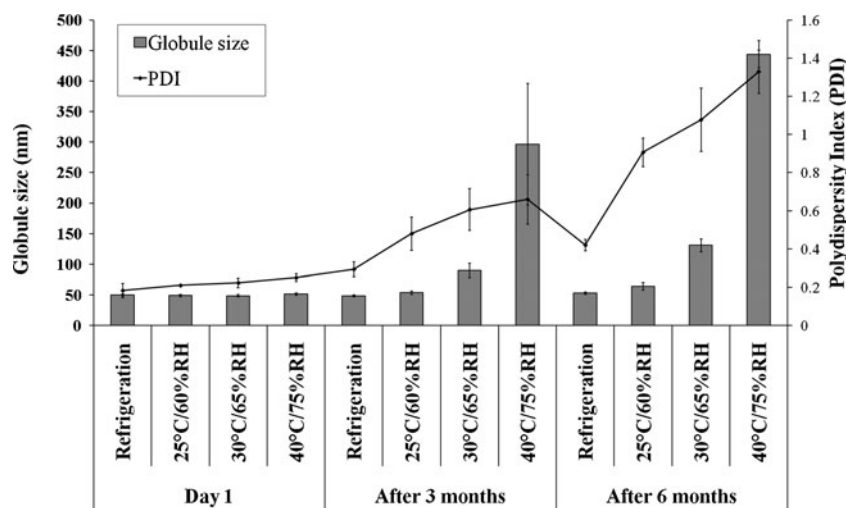


respectively. Thus, lower value of PPE (<5) indicates robustness of the mathematical model and high prognostic ability of the experimental design.

Physicochemical characterization of MEI and MBGI

The globules of MEI appeared to be almost round in shape in transmission electron microscope. The globule appeared dark in bright surroundings (Fig. 5). The average droplet size of MEI was 48.3 nm with polydispersity index (PDI) of 0.19. The PDI value close to zero shows that MEI globules were homogenous and had narrow size distribution. The transparency of MEI was proved by refractive index 1.39 and >99 % transmittance. Further, MEI formulation was observed as completely dark under cross polarizer, which implies that MEI was optically isotropic and was colloidal dispersion. The conductivity of the formulation was $138.3 \pm 2.4 \mu\text{scm}^{-1}$, which confirmed the o/w nature of MEI. The structural composition of MEI was evaluated using DRIFTS technique. FTIR spectra of MEI, IPM, oleic acid, and IT are shown in Fig. 6. Itraconazole showed characteristic peaks at 3,381, 3,126, 3,069, 2,964, 2,823, 1,697, 1,510, and 1,450 cm^{-1} . The sharp peak obtained at 1,697 is due to C=O of IT. The characteristic peaks at 1,609 and 1,425 are due to C=N and C–N, respectively. The oil components viz. oleic acid and IPM showed characteristic peaks at 2,924, 2,854, and 1,747. In MEI, the characteristic peaks of IT are absent but peaks of oleic acid and IPM are present. Similar kind of results were obtained and reported by Pople et al. with Tacrolimus-loaded modified nano lipid carrier [35]. Absence of IT peaks in MEI could be attributed to complete solubilization and/or encapsulation of IT in oil phase [44]. Further, FTIR spectra of MEI did not show any new peak confirming no interaction or incompatibility in the developed formulation.

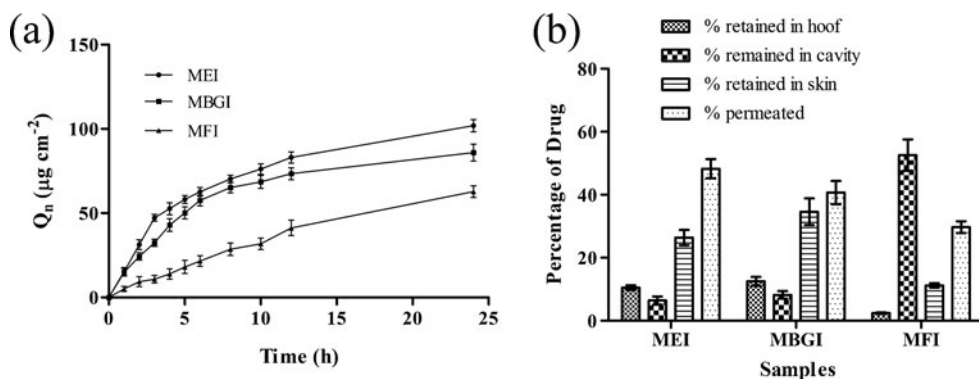
Fig. 7 Stability profile of MEI as per ICH guidelines indicating globule size (nanometer) and PDI (mean \pm SD, $n=3$)



MBGI was obtained by addition of 0.7 % Carbopol 934P, to render it suitable for application in to the cavity between nail plate and nail bed. The concentration of carbopol 934P was selected from the preliminary experiments, which were carried out with a view to get the appropriate viscosity for application in ventral edges of nail, so that the gel could not be drained out. The viscosity of MBGI (21.24 ± 0.24 Pas) increased significantly as compared to MEI (43.57 ± 0.28 mPas). The yield stress of MBGI was 1.2 Pas indicating good spreadability and pourability at minimum pressure.

The pH values of MEI and MBGI were 5.2 and 6.82, respectively, which implies that MBGI has less stimulating capacity than MEI [45, 46]. The optimized MEI formulation and MBGI had IT loading of 12.3 and 0.5 % w/w, respectively. Samples of MEI and MBGI remained stable over a period of 6 months with no change in their physical appearance. The MEI samples showed insignificant changes in the globule size and PDI at refrigeration and at 25 °C/60 % RH but significant changes ($P > 0.05$) at high temperature storage conditions (30 °C/65 % RH and 40 °C/75 % RH; Fig. 7). At refrigeration conditions, the globule size remained between 49.66 ± 2.08 and 52.66 ± 2.08 nm and at 25 °C/60 % RH it remained between 49 ± 2 and 64 ± 6.24 nm. At higher temperature storage conditions, the globule size varied from 48.66 ± 2.08 to 444 ± 22.11 nm suggesting unstable behavior. Similarly, PDI values were constant for all the samples at refrigeration and at 25 °C/60 % RH but drastically changed during higher temperature storage conditions. Thus, MEI and MBGI could be considered stable at refrigeration and at 25 °C/60 % RH. At higher temperatures microemulsion globules tend to coalesce resulting in creaming and breaking of microemulsion.

Fig. 8 a Permeation profiles of tested formulations (mean±SD, $n=3$); **b** mass balance of IT in different compartments after the in vitro permeation study (mean±SD, $n=3$)



Ex vivo permeation studies

The permeation profile (Fig. 8a) was obtained by placing optimized MEI formulation, MFI and MBGI (each containing 20 mg IT) between the bovine hoof membrane and human cadaver skin between the donor and receiver compartments in the Franz diffusion cell. It was observed that IT concentration steadily increased in the receptor chamber with increase in time, where the permeation profile generally followed Fick's diffusion law. The cumulative amount of IT permeated (Q_n) from MEI, MBGI, and MFI at 12 h after application were 83.02 ± 3.27 , 73.39 ± 3.55 , and 41.23 ± 4.54 $\mu\text{g cm}^{-2}$, respectively. The comparatively higher Q_n of MEI and MBGI could be due to increased diffusion coefficient of drug [47, 48]. Moreover, smaller globule size of optimized microemulsion provides larger area for permeation of drug in to skin and high drug concentration on the affected area results in a larger concentration gradient, which is a necessity for efficient dermal drug delivery. The amount of drug lost in the sample inserted during the permeation study was considered while calculating percentage drug permeated.

After the permeation study of 24 h, the percentage drug present in the cavity between the bovine hoof membrane and the skin was determined by washing it three to four times with the physiological saline solution. The solution was filtered through a 0.22- μm filter and was analyzed by HPLC for the drug content. For estimating the drug retained in the skin and hoof membrane, the skin, and hoof were cut into small pieces and was kept in the physiological saline solution (pH5.5 acetate buffer: methanol (9:1)) for 24 h, which was then sonicated in the ultrasonicator for 10 min followed by vortex mixing for 15 min. The samples were then centrifuged at 6,000 rpm for 15 min. After centrifugation, supernatant was taken, filtered through a 0.22- μm filter and was analyzed for the drug content. Figure 7b shows the partitioning of drug into different compartments of skin and hoof. The permeation was observed maximum with MEI (48.26 ± 5.21 %) followed by MBGI (40.67 ± 6.40 %). The commercial cream (MFI) which was used as a control had large amount of the drug in the cavity (52.6 ± 8.63 %), which was neither permeated nor retained in hoof membrane or

skin. MBGI showed maximum retention of the drug in both bovine hoof membrane (12.5 ± 2.46 %) and skin (34.6 ± 7.34 %), which was due to increased viscosity of the MBGI, converting the optimized microemulsion into lamellar structure or a highly ordered microstructure [49, 50]. High viscosity of MFI prevents the migration of drug from the cream to nail plate and nail bed. On the contrary, viscosity of MBGI is such that it is easy to apply in the onycholytic cavity. Moreover, MBGI allows microemulsion globules containing drug to penetrate into the layers of nail bed and nail plate for effective antifungal action. The killing of nail fungus could be possible only if larger amount of drug retains into the nail and skin layers. Thus, MBGI could be a promising drug delivery vehicle for the treatment of onychomycosis.

Ex vivo antifungal study

Ex vivo antifungal study was carried with optimized MBGI, MFI, and control. For both the strains (*C. albicans* and *T. rubrum*), mean zone of inhibition was calculated, which was taken as an indicator for the antifungal activity. It was observed that MBGI was more effective in killing the fungus as compared to MFI (Table 3). Significant difference was observed at 5 % level of significance between zone of inhibition diameters of MBGI and control, MFI and control, MBGI and MFI ($P<0.05$). The smaller globule size of optimized MEI results in better diffusion of the drug through the barriers. Moreover, MBGI has very low interfacial tension and large interfacial area; so larger amount of drug could be concentrated

Table 3 Zone of inhibition diameter for MBGI and MFI

Samples	Mean zone of inhibition diameter (mm)	
	<i>C. albicans</i>	<i>T. rubrum</i>
MBGI	32.54 ± 2.74	27.89 ± 1.26
MFI	14.46 ± 2.41	19.27 ± 1.66

^a Mean of 3±SD

and localized within the same isotropic medium, thus providing enhanced antifungal action as compared to MFI.

Conclusions

In this research paper, the microemulsion components were optimized using D-optimal design to get the optimum globule size and drug loading. The results showed that microemulsion components had significant effect on the responses. The formulation containing 6.24 % oleic acid+IPM (1:1), 26.99 % Labrasol, 8.99 %, Transcutol P, and 57.76 % water was selected as an optimized formulation which provided globule size 48.2 nm and drug loading 12.13 mg/ml. The drug-loaded gel (MBGI) showed better retention in the bovine hoof and human cadaver skin and an enhanced antifungal activity as compared to market formulation (MFI), which could be due to special characteristics of microemulsion. Thus, the drug-loaded gel could be a promising formulation to reduce the symptoms and to cure onychomycosis faster than the conventional therapies.

Acknowledgments The authors are thankful to Cadila Pharmaceuticals Ltd. (Ahmedabad, India) for providing Itraconazole; Abitec Corporation (Ohio, USA) for providing Capmul MCM; and Gattefosse (Lyon, France) for providing the free samples of Labrasol, Labrafac, and Transcutol P. The authors are also thankful to Institute of Microbial Technology (Chandigarh, India) for providing the fungal strains. The authors are grateful to Mrs. Mallika Babu for proofreading the manuscript for grammatical and spelling errors. This study is a part of research project, carried out at Kadi Sarva Vishwavidyalaya (Gandhinagar, India).

References

- Gupta AK, Simpson FC. New therapeutic options for onychomycosis. *Expert Opin Pharmacother.* 2012;13(8):1131–42.
- Grover C, Khurana A. Onychomycosis: newer insights in pathogenesis and diagnosis. *Indian J Dermatol Venereol Leprol.* 2012;78(3):263–70.
- Baran R, Kaoukhov A. Topical antifungal drugs for the treatment of onychomycosis: an overview of current strategies for monotherapy and combination therapy. *J Eur Acad Dermatol Venereol.* 2005;19:21–9.
- Baran R, Gupta AK, Pierard GE. Pharmacotherapy of onychomycosis. *Expert Opin Pharmacother.* 2005;6(4):609–24.
- Arrese JE, Pierard GE. Treatment failures and relapses in onychomycosis: a stubborn clinical problem. *Dermatology.* 2003;207(3):255–60.
- Kobayashi Y, Miyamoto M, Sugibayashi K, Morimoto Y. Drug permeation through the three layers of the human nail plate. *J Pharm Pharmacol.* 1999;51(3):271–8.
- Murdan S. Drug delivery to the nail following topical application. *Int J Pharm.* 2002;236(1–2):1–26.
- Amichai B, Nitzan B, Mosckovitz R, Shemer A. Iontophoretic delivery of terbinafine in onychomycosis: a preliminary study. *Br J Dermatol.* 2010;162(1):46–50.
- Sachdeva V, Siddoju S, Yu YY, Kim HD, Friden PM, Banga AK. Transdermal iontophoretic delivery of terbinafine hydrochloride: quantitation of drug levels in stratum corneum and underlying skin. *Int J Pharm.* 2010;388(1–2):24–31.
- Nair AB, Vaka SR, Sammeta SM, Kim HD, Friden PM, Chakraborty B, et al. Trans-ungual iontophoretic delivery of terbinafine. *J Pharm Sci.* 2009;98(5):1788–96.
- Murdan S. Enhancing the nail permeability of topically applied drugs. *Expert Opin Drug Deliv.* 2008;5(11):1267–82.
- Barot BS, Parejiya PB, Patel HK, Gohel MC, Shelat PK. Microemulsion-based gel of terbinafine for the treatment of onychomycosis: optimization of formulation using D-optimal design. *AAPS PharmSciTech.* 2012;13(1):184–92.
- Heuschkel S, Goebel A, Neubert RHH. Microemulsions-modern colloidal carrier for dermal and transdermal drug delivery. *J Pharm Sci.* 2008;97(2):603–31.
- Lawrence MJ, Rees GD. Microemulsion-based media as novel drug delivery systems. *Adv Drug Deliv Rev.* 2000;45(1):89–121.
- Ghosh PK, Murthy RS. Microemulsions: a potential drug delivery system. *Curr Drug Deliv.* 2006;3(2):167–80.
- Kreilgaard M. Influence of microemulsions on cutaneous drug delivery. *Adv Drug Deliv Rev.* 2002;54 Suppl 1:S77–98.
- Zhu W, Yu A, Wang W, Dong R, Wu J, Zhai G. Formulation design of microemulsion for dermal delivery of penciclovir. *Int J Pharm.* 2008;360(1–2):184–90.
- Raza K, Negi P, Takyar S, Shukla A, Amarji B, Katare OP. Novel dithranol phospholipid microemulsion for topical application: development, characterization and percutaneous absorption studies. *J Microencapsul.* 2011;28(3):190–9.
- Patel HK, Barot BS, Parejiya PB, Shelat PK, Shukla A. Topical delivery of clobetasol propionate loaded microemulsion based gel for effective treatment of vitiligo: ex vivo permeation and skin irritation studies. *Colloids Surf B Biointerfaces.* 2013;102(2):86–94.
- Zhu W, Guo C, Yu A, Gao Y, Cao F, Zhai G. Microemulsion-based hydrogel formulation of penciclovir for topical delivery. *Int J Pharm.* 2009;378(1–2):152–8.
- Mertin D, Lippold BC. In-vitro permeability of the human nail and of a keratin membrane from bovine hooves: prediction of the penetration rate of antimycotics through the nail plate and their efficacy. *J Pharm Pharmacol.* 1997;49(9):866–72.
- Khengar RH, Jones SA, Turner RB, Forbes B, Brown MB. Nail swelling as a pre-formulation screen for the selection and optimization of unguinal penetration enhancers. *Pharm Res.* 2007;24(12):2207–12.
- Nair AB, Sammeta SM, Kim HD, Chakraborty B, Friden PM, Murthy SN. Alteration of the diffusional barrier property of the nail leads to greater terbinafine drug loading and permeation. *Int J Pharm.* 2009;375(1–2):22–7.
- Hao J, Smith KA, Li SK. Iontophoretically enhanced ciclopirox delivery into and across human nail plate. *J Pharm Sci.* 2009;98(10):3608–16.
- Kumar S, Kimball AB. New antifungal therapies for the treatment of onychomycosis. *Expert Opin Investig Drugs.* 2009;18(6):727–34.
- Nair AB, Kiran Vaka SR, Murthy SN. Transungual delivery of terbinafine by iontophoresis in onychomycotic nails. *Drug Dev Ind Pharm.* 2011;37(10):1253–8.
- Gupta AK, De Doncker P, Scher RK, Haneke E, Daniel 3rd CR, Andre J, et al. Itraconazole for the treatment of onychomycosis. *Int J Dermatol.* 1998;37(4):303–8.
- Kawakami K, Yoshikawa T, Moroto Y, Kanaoka E, Takahashi K, Nishihara Y, et al. Microemulsion formulation for enhanced absorption of poorly soluble drugs. I. Prescription design. *J Control Release.* 2002;81(1–2):65–74.
- Leucuta SE, Bodea A. Optimization of hydrophilic matrix tablets using a D-optimal design. *Int J Pharm.* 1997;153(2):247–55.

30. Holm R, Jensen IH, Sonnergaard J. Optimization of self-microemulsifying drug delivery systems (SMEDDS) using a D-optimal design and the desirability function. *Drug Dev Ind Pharm.* 2006;32(9):1025–32.
31. Lewis GA, Mathieu D, Phan-Tan-Luu R. Mixtures in a constrained region of interest. In: Swarbrick J, editor. *Pharmaceutical experimental design.* New York: Marcel Dekker, Inc.; 1999. p. 413–54.
32. Basketter DA, York M, McFadden JP, Robinson MK. Determination of skin irritation potential in the human 4-h patch test. *Contact Dermatitis.* 2004;51(1):1–4.
33. Boelsma E, Tanojo H, Bodde HE, Ponc M. Assessment of the potential irritancy of oleic acid on human skin: evaluation in vitro and in vivo. *Toxicol In Vitro.* 1996;10(6):729–42.
34. Barik B, Panigrahi L, Maharana L, Ghosal SK, Pattnaik S. Effect of permeation enhancers on the release and permeation kinetics of Lincomycin hydrochloride gel formulations through mouse skin. *Ind J Pharm Sci.* 2006;68(2):205–11.
35. Pople PV, Singh KK. Targeting tacrolimus to deeper layers of skin with improved safety for treatment of atopic dermatitis. *Int J Pharm.* 2010;398(1–2):165–78.
36. Hui X, Wester RC, Maibach HI, Barbadillo S. Nail penetration—enhance topical delivery of antifungal drugs by chemical modification of the human nail. In: Bronaugh RL, Maibach HI, editors. *Percutaneous absorption: drugs-cosmetics-mechanisms-methodology.* 4th ed. Boca Raton: Taylor & Francis; 2005. p. 643–53.
37. Monti D, Saccomani L, Chetoni P, Burgalassi S, Tampucci S, Mailland F. Validation of bovine hoof slices as a model for infected human toenails: in vitro ciclopirox transungual permeation. *Br J Dermatol.* 2011;165(1):99–105.
38. Redmann S, Charles BG. A rapid HPLC method with fluorometric detection for determination of plasma itraconazole and hydroxy-itraconazole concentrations in cystic fibrosis children with allergic bronchopulmonary aspergillosis. *Biomed Chromatogr.* 2006;20(4):343–8.
39. Larrucea E, Arellano A, Santoyo S, Ygartua P. Combined effect of oleic acid and propylene glycol on the percutaneous penetration of tenoxicam and its retention in the skin. *Eur J Pharm Biopharm.* 2001;52(2):113–9.
40. Hua L, Weisan P, Jiayu L, Ying Z. Preparation, evaluation, and NMR characterization of vinpocetine microemulsion for transdermal delivery. *Drug Dev Ind Pharm.* 2004;30(6):657–66.
41. Li H, Pan WS, Wu Z, Li JY, Xia LX. Optimization of microemulsion containing vinpocetine and its physicochemical properties. *Yao Xue Xue Bao.* 2004;39(9):681–5.
42. Shafiq-un-Nabi S, Shakeel F, Talegaonkar S, Ali J, Baboota S, Ahuja A, et al. Formulation development and optimization using nanoemulsion technique: a technical note. *AAPS PharmSciTech.* 2007;8(2):E12–7.
43. Ceschel G, Bergamante V, Maffei P, Borgia SL, Calabrese V, Biserni S, et al. Solubility and transdermal permeation properties of a dehydroepiandrosterone cyclodextrin complex from hydrophilic and lipophilic vehicles. *Drug Deliv.* 2005;12(5):275–80.
44. Jain S, Mistry MA, Swarnakar NK. Enhanced dermal delivery of acyclovir using solid lipid nanoparticles. *Drug Deliv and Transl Res.* 2011;1:395–406.
45. Chen H, Chang X, Du D, Li J, Xu H, Yang X. Microemulsion-based hydrogel formulation of ibuprofen for topical delivery. *Int J Pharm.* 2006;315(1–2):52–8.
46. Chen H, Mou D, Du D, Chang X, Zhu D, Liu J, et al. Hydrogel-thickened microemulsion for topical administration of drug molecule at an extremely low concentration. *Int J Pharm.* 2007;341(1–2):78–84.
47. El Maghraby GM. Transdermal delivery of hydrocortisone from eucalyptus oil microemulsion: effects of cosurfactants. *Int J Pharm.* 2008;355(1–2):285–92.
48. Huang YB, Lin YH, Lu TM, Wang RJ, Tsai YH, Wu PC. Transdermal delivery of capsaicin derivative-sodium nonivamide acetate using microemulsions as vehicles. *Int J Pharm.* 2008;349(1–2):206–11.
49. Peltola S, Saarinen-Savolainen P, Kiesvaara J, Suhonen TM, Urtti A. Microemulsions for topical delivery of estradiol. *Int J Pharm.* 2003;254(2):99–107.
50. Trotta M. Influence of phase transformation on indomethacin release from microemulsions. *J Control Release.* 1999;60(2–3):399–405.